

# Synthesis, Excited-State Dynamics, and Reactivity of a Directly-Linked Pyromellitimide–(Porphinato)zinc(II) Complex

Naomi P. Redmore, Igor V. Rubtsov, and Michael J. Therien\*

Department of Chemistry, University of Pennsylvania, Philadelphia, Pennsylvania 19104-6323

Received August 9, 2001

*N*-[5-(10,20-Diphenylporphinato)zinc(II)]–*N'*-(octyl)pyromellitic diimide (PZn–PI), a *meso*-pyromellitimide-substituted (porphinato)zinc(II) compound, has been fabricated from the reaction of (5-amino-10,20-diphenylporphinato)zinc(II) with pyromellitic dianhydride in the presence of octylamine. Interrogation of the photoinduced charge separation (CS) and thermal charge recombination (CR) electron-transfer (ET) dynamics for PZn–PI in CH<sub>2</sub>Cl<sub>2</sub> via pump–probe transient absorption spectroscopic methods shows that  $\tau_{CS}$  and  $\tau_{CR}$  are 770 and 5200 fs, respectively. These ET dynamics differ from those elucidated previously for closely related 5-quinonyl-substituted (porphinato)-metal compounds, and derive from the fact that the low-lying excited states for PZn–PI are porphyrin-localized, possessing little charge-transfer character. The synthesis of *N*-{5-[15-(2-(triisopropylsilyl)ethynyl)-10,20-diphenylporphinato]zinc(II)}–*N'*-(octyl)pyromellitic diimide demonstrates that PZn–PI can be halogenated at its 15-*meso*-position and used subsequently as a substrate in metal-catalyzed cross-coupling reactions; the reactivity of PZn–PI is unusual with respect to many directly linked donor–acceptor compounds in that it is stable to these oxidizing and reducing reaction conditions.

## Introduction

Ultrafast electron-transfer (ET) events play important roles in nature. During photosynthesis, fast, multistep ET reactions transform the energy of absorbed light into chemical potential energy with near unit efficiency. Porphyrin–quinone (P–Q) compounds, in which the quinone is directly fused to the porphyrin macrocycle, have served as benchmark systems with which to probe biologically relevant, photoinduced charge separation (CS) and thermal charge recombination (CR) reactions that involve strong donor–acceptor (D–A) electronic coupling.<sup>1–10</sup>

We report the synthesis of a closely related D–A system (PZn–PI) in which a pyromellitimide (PI) acceptor is directly linked to the *meso*-carbon of a (porphinato)zinc(II) (PZn) chromophore, and contrast its ET dynamics with those established previously for its P–Q counterpart. We also show that this complex is amenable to subsequent functionalization, enabling this D–A unit to serve as a key building block for the synthesis of more complex ET assemblies.

## Experimental Section

**Materials.** All manipulations were carried out under nitrogen prepurified by passage through an O<sub>2</sub> scrubbing tower (Schweizerhall R3-11 catalyst) and a drying tower (Linde 3 Å molecular sieves) unless otherwise stated. Air-sensitive solids were handled in a Braun 150-M glovebox. Standard Schlenk techniques were employed to manipulate air-sensitive solutions, while solvents utilized in this work were obtained from Fisher Scientific (HPLC grade). Tetrahydrofuran (THF) was distilled from K/benzoylbiphenyl. Pd(PPh<sub>3</sub>)<sub>4</sub> (Strem or Aldrich) was used as received. Chromatographic purification (silica gel 60, 230–400 mesh, EM Science, and Bio-Beads S-X1, 200–400 mesh, BioRad) of all newly synthesized compounds was accomplished on the benchtop. Chemical shifts for <sup>1</sup>H NMR spectra are relative to residual protium in the deuterated solvents (CDCl<sub>3</sub>,  $\delta$  = 7.24 ppm). All coupling constants are reported in

\* To whom correspondence should be addressed. E-mail: therien@chem.upenn.edu.

- (1) Wynne, K.; LeCours, S. M.; Galli, C.; Therien, M. J.; Hochstrasser, R. M. *J. Am. Chem. Soc.* **1995**, *117*, 3749–3753.
- (2) Wasielewski, M. R. *Chem. Rev.* **1992**, *92*, 435–461.
- (3) Gust, D.; Moore, T. A. *Top. Curr. Chem.* **1991**, *159*, 103–151.
- (4) Sumida, J. P.; Liddell, P. A.; Lin, S.; Macpherson, A. N.; Seely, G. R.; Moore, A. L.; Moore, T. A.; Gust, D. *J. Phys. Chem. A* **1998**, *102*, 5512–5519.
- (5) Rodriguez, J.; Kirmaier, C.; Johnson, M. R.; Friesner, R. A.; Holten, D.; Sessler, J. L. *J. Am. Chem. Soc.* **1991**, *113*, 1652–1659.
- (6) Sessler, J. L.; Capuano, V. L.; Harriman, A. *J. Am. Chem. Soc.* **1993**, *115*, 4618–4628.
- (7) Dalton, J.; Milgrom, L. R. *J. Chem. Soc., Chem. Commun.* **1979**, 609–610.
- (8) Bergkamp, M. A.; Dalton, J.; Netzel, T. L. *J. Am. Chem. Soc.* **1982**, *104*, 253–259.
- (9) Cormier, R. A.; Posey, M. R.; Bell, W. L.; Fonda, H. N.; Connolly, J. S. *Tetrahedron* **1989**, *45*, 4831–4843.

- (10) D'Souza, F.; Deviprasad, G. R.; Hsieh, Y.-Y. *Chem. Commun.* **1997**, 533–534.

hertz. Mass spectra were obtained at the University of Pennsylvania Mass Spectrometry Laboratory.

**Instrumentation.** NMR spectra were recorded on a 250 MHz AC-Bruker spectrometer. Electronic spectra were obtained on an OLIS UV/vis/near-IR spectrophotometry system that is based on the optics of a Cary 14 spectrophotometer. Uncorrected static fluorescence emission spectra were recorded on a Perkin-Elmer LS-50 luminescence spectrometer.

Cyclic voltammetric responses were obtained using an EG&G Princeton Applied Research model 273A potentiostat/galvanostat. The components of the electrochemical cell included a glassy carbon working electrode, a Pt wire counter electrode, and a saturated calomel (SCE) reference electrode. The potential of the ferrocene/ferrocenium redox couple (0.4 V vs SCE) was used as an internal redox standard.

**Pump–Probe Transient Absorption Spectroscopic Measurements.** Transient absorption spectra were obtained using standard pump–probe methods. Optical pulses, centered at 775 nm, were generated using a Ti:sapphire laser (Clark-MXR, CPA-2001). Optical parametric amplifiers (near-IR and visible OPAs, Clark-MXR) generate excitation pulses tunable in wavelength from the UV through the near-IR region; a white light continuum served as the probe beam. After passing through the sample, the probe light was focused onto the entrance slit of the computer-controlled image spectrometer (SpectraPro-150, Acton Research Corp.). The noise level in these transient absorption experiments corresponded to ~0.2 mOD/s of signal accumulation. The time resolution is probe wavelength dependent; in these experiments the fwhm of the instrument response function varied between 140 and 200 fs. A detailed description of the transient optical apparatus will appear in an upcoming paper.<sup>11</sup> All experiments were carried out at room temperature (23 ± 1 °C).

***N*-[5-(10,20-Diphenylporphinato)zinc(II)]-*N'*-(Octyl)pyromellitic Diimide (PZn–PI).** (5-Amino-10,20-diphenylporphinato)zinc(II) (210 mg, 400 μmol), octylamine (130 μL, 800 μmol), and pyromellitic dianhydride (131 mg, 600 μmol) were added to a 100 mL Schlenk tube charged with anhydrous dimethylformamide (50 mL). The resultant solution was stirred under N<sub>2</sub> at reflux for 13 h. After being cooled to room temperature, the reaction mixture was diluted with chloroform (100 mL) and washed with deionized water (3 × 50 mL). After the organic solution was dried over sodium sulfate, the solvent was removed by distillation under vacuum, and the residue chromatographed on silica gel (1:1 hexanes/THF). The first fraction eluted as a mixture of PZn–PI and (10,20-diphenylporphinato)zinc(II). Gel permeation chromatography (THF) was required to separate these compounds; the first eluted fraction corresponded to PZn–PI (41 mg, 12% based on 400 μmol of (5-amino-10,20-diphenylporphinato)zinc(II)). <sup>1</sup>H NMR (250 MHz, CDCl<sub>3</sub>/pyr-*d*<sub>5</sub>): δ 0.83 (5 H, m, CH<sub>3</sub>, CH<sub>2</sub>), 1.3 (8 H, m, CH<sub>2</sub>), 1.8 (2 H, m, CH<sub>2</sub>), 3.7 (2 H, t, CH<sub>2</sub>), 7.7 (6 H, m, Ar H), 8.1 (4 H, m, Ar H), 8.6 (2 H, s, Ar<sub>pyrom</sub> H), 8.9 (6 H, m, β-H), 9.3 (2 H, d, *J* = 4.5 Hz, β-H), 10.2 (1 H, s, *meso*-H). Vis (CH<sub>2</sub>Cl<sub>2</sub>): λ<sub>max</sub> (nm) (log ε (M<sup>-1</sup> cm<sup>-1</sup>)): 412 (5.58), 540 (4.15). ESMS: *m/z* 850.2232 (calcd 850.2246).

***N*-[5-(15-Bromo-10,20-diphenylporphinato)zinc(II)]-*N'*-(Octyl)pyromellitic Diimide (3).** *N*-Bromosuccinimide (5 mg, 26 μmol) in anhydrous methylene chloride (5 mL) was added dropwise under N<sub>2</sub> to a solution of PZn–PI (24 mg, 28 μmol) in anhydrous methylene chloride (10 mL). The mixture was stirred at room temperature for 5 min, quenched by the addition of acetone (1 mL),

washed with water, and dried over sodium sulfate. Removal of volatiles yielded a purple solid which was chromatographed on silica gel (CHCl<sub>3</sub>) to yield **3** (24 mg, 99% based on 5 mg of *N*-bromosuccinimide). <sup>1</sup>H NMR (250 MHz, CDCl<sub>3</sub>/pyr-*d*<sub>5</sub>): δ 0.86 (5 H, m, CH<sub>3</sub>, CH<sub>2</sub>), 1.3 (8 H, m, CH<sub>2</sub>), 1.7 (2 H, m, CH<sub>2</sub>), 3.7 (2 H, t, CH<sub>2</sub>), 7.7 (6 H, m, Ar H), 8.1 (4 H, m, Ar H), 8.6 (2 H, s, Ar<sub>pyrom</sub> H), 8.9 (6 H, m, β-H), 9.7 (2 H, d, β-H). Vis (CH<sub>2</sub>Cl<sub>2</sub>): λ<sub>max</sub> (nm) 422, 552, 592. ESMS: *m/z* 928.1364 (calcd 928.1351).

***N*-[5-[15-(2-(Triisopropylsilyl)ethynyl)-10,20-diphenylporphinato]zinc(II)]-*N'*-(Octyl)pyromellitic Diimide (4).** A solution of (trimethylsilyl)acetylene (70 μL, 520 μmol) in dry, degassed THF (50 mL) was cooled to –78 °C under N<sub>2</sub>. *n*-Butyllithium (570 μmol, 1.6 M in hexanes, 360 μL) was added dropwise with stirring, and the resultant solution was warmed to room temperature. Zinc chloride (180 mg, 1.29 mmol) was added under a rapid flow of N<sub>2</sub>, and the mixture was stirred for 10 min. A portion (5 mL, 50 μmol, 1.0 μM) of the resultant solution was removed with a gastight syringe and added to a 25 mL Schlenk tube charged with **3** (24 mg, 25.8 μmol) and Pd(Ph<sub>3</sub>)<sub>4</sub> (1.0 mg, 1.0 μmol, 5%) in dry, degassed THF (5 mL). After the mixture was stirred under nitrogen for 4 h, TLC (CHCl<sub>3</sub>) indicated that the reaction was complete. The reaction mixture was then diluted with ethyl acetate (25 mL), washed with water, dried over calcium chloride, and evaporated. The recovered residue was purified by column chromatography (CHCl<sub>3</sub>) to give **4** (22 mg, 89% based on 24 mg of **3**). <sup>1</sup>H NMR (250 MHz, CDCl<sub>3</sub>): δ 0.59 (9 H, s, SiCH<sub>3</sub>), 0.88 (5 H, m, CH<sub>3</sub>–CH<sub>2</sub>), 1.3 (6 H, m, CH<sub>2</sub>), 1.8 (2 H, m, CH<sub>2</sub>), 3.8 (2 H, t, CH<sub>2</sub>), 7.7 (6 H, m, Ar H), 8.1 (4 H, m, Ar H), 8.6 (2 H, s, Ar<sub>pyrom</sub> H), 8.9 (6 H, m, β-H), 9.7 (2 H, d, *J* = 4.5 Hz, β-H). Vis (EtOAc): λ<sub>max</sub> (nm) 430, 564, 612. ESMS: *m/z* 947.2680 (calcd 947.2720).

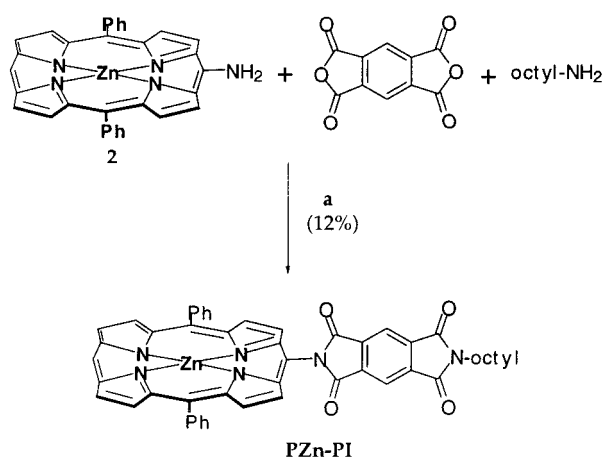
## Results and Discussion

The D–A dyad *N*-[5-(10,20-diphenylporphinato)zinc(II)]-*N'*-(octyl)pyromellitic diimide (PZn–PI) was prepared in three steps from (10,20-diphenylporphinato)zinc(II) (**1**). Nitration of **1** was accomplished regioselectively with iodine and silver nitrite, affording (5-nitro-10,20-diphenylporphinato)zinc(II) in high yield.<sup>12,13</sup> This (*meso*-nitroporphinato)zinc(II) complex was then reduced to the corresponding amino derivative (5-amino-10,20-diphenylporphinato)zinc(II) (**2**) with sodium borohydride and 10% Pd on carbon catalyst.<sup>12,13</sup> PZn–PI was prepared via the one-pot cyclization reaction of **2** and octylamine with pyromellitic dianhydride, as shown in Scheme 1.

Early work by Sanders and Osuka<sup>14,15</sup> established the utility of the PI acceptor in porphyrin-based donor–spacer–acceptor (D–Sp–A) assemblies. This species is a strong electron acceptor [*E*<sup>1/2</sup>(PI<sup>•–</sup>/PI) = –0.8 V vs SCE]<sup>16</sup> that features a radical anion absorbance with significant oscillator strength (λ = 710 nm). The PI moiety thus provides a spectral signature for monitoring the growth and decay of ET intermediates independent of the porphyrin ground–

(11) Rubtsov, I. V.; Kang, Y. K.; Rubtsov, G. I.; Therien, M. J. Manuscript in preparation.

- (12) Baldwin, J. E.; DeBernardis, J. F. *J. Org. Chem.* **1977**, *42*, 3986–3987.
- (13) Baldwin, J. E.; Crossley, M. J.; DeBernardis, J. *Tetrahedron* **1982**, *38*, 685–692.
- (14) Hunter, C. A.; Sanders, J. K. M.; Beddard, G. S.; Evans, S. *J. Chem. Soc., Chem. Commun.* **1989**, 1765–1767.
- (15) Osuka, A.; Nakajima, S.; Maruyama, K.; Mataga, N.; Asahi, T. *Chem. Lett.* **1991**, 1003–1006.
- (16) Wiederrecht, G. P.; Svec, W. A.; Niemczyk, M. P.; Wasielewski, M. R. *J. Phys. Chem.* **1995**, *99*, 8918–8926.

Scheme 1<sup>a</sup>

<sup>a</sup> Conditions: (a) refluxing DMF.

excited-, and cation-radical-state spectral features. Numerous studies have demonstrated the value of the PI acceptor for probing multistep charge-transfer processes in a variety of synthetic ET assemblies.<sup>16–20</sup>

The electronic spectrum of PZn–PI corresponds to that observed for **1** (see the Supporting Information), demonstrating that the perturbation to the porphyrin  $S_0$ ,  $S_1$ , and  $S_2$  electronic states upon appendage of the PI acceptor to the (porphyrinato)zinc(II) chromophore is not severe. This observation is in marked contrast to analogous optical spectra obtained for P–Q systems in which a quinonyl unit is fused directly to the porphyrin macrocycle.<sup>1</sup>

The photoinduced and thermal charge recombination ET dynamics of PZn–PI in  $\text{CH}_2\text{Cl}_2$  were investigated by pump–probe transient absorption spectroscopy (Figure 1). PZn–PI was excited by a 120 fs pulse ( $\lambda = 549 \text{ nm}$ ), resulting in the formation of a porphyrin-based doubly degenerate singlet excited state [ $^1(\text{PZn})^*-\text{PI}$ , Figure 2]. The subsequent charge separation reaction can be fit as a monoexponential process with a time constant  $\tau_{\text{CS}}$  of 770 fs. The transient absorption spectrum corresponding to a time delay of 2.0 ps (Figure 1) displays the classic spectral signatures for both the PI anion radical<sup>15</sup> and the PZn cation radical;<sup>21</sup> note that the characteristic respective absorbances (710 and 470 nm) for these two species are clearly evident. This charge-separated state undergoes a rapid charge recombination reaction ( $\tau_{\text{CR}} = 5.2 \text{ ps}$ ), producing a vibrationally hot ground state. The hot ground state cools with a time constant of 17 ps in methylene chloride, similar to that observed for strongly coupled PQ benchmarks.<sup>5</sup> It is important to note that similar transient dynamics are observed for PZn–PI irrespective of the excitation wavelength within the Q-state absorption manifold.

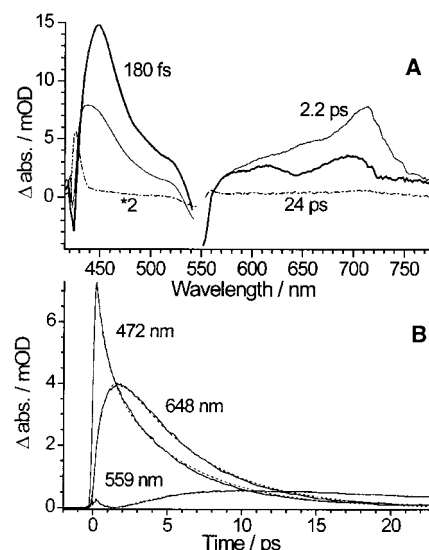


**Figure 1.** (A) Transient absorbance spectra obtained following excitation of PZn–PI at 549 nm measured at the labeled time delays. Experimental conditions: solvent, methylene chloride; temperature, 23 °C. (B) Exemplary wavelength-dependent transient decays. A global fit of the data, using three exponential functions, gives  $\tau_{\text{CS}}$  (charge separation) = 770 fs,  $\tau_{\text{CR}} = 5.2 \text{ ps}$ ,  $\tau_{\text{vibrational cooling}}$  (of the hot ground state formed following charge recombination) = 17 ps.

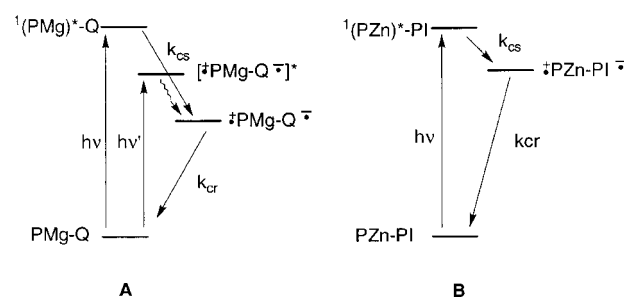


**Figure 2.** Summary of the proposed electron-transfer dynamics for (A) PMg–Q and (B) PZn–PI.

It is instructive to compare the ET dynamics manifest by PZn–PI with that displayed by a related P–Q compound, (5-quinonyl-10,15,20-triphenylporphyrinato)magnesium(II) (PMg–Q). Ultrafast time-resolved spectroscopy demonstrates extensive mixing between the quinone moiety and the (porphyrinato)metal  $x$ -polarized Q state.<sup>1</sup> Excitation within the  $Q_x$  absorption band ( $h\nu'$ , Figure 2A) produces a charge-transfer (CT) excited state, [ $\text{P}^+\text{Mg}-\text{Q}^-$ ]\*, which decays via rapid internal conversion to a vibrationally relaxed CT state ( $\text{P}^+\text{Mg}-\text{Q}^-$ , Figure 2A) within a subpicosecond time domain.<sup>1</sup> In contrast, electronic excitation within the  $Q_y$  absorption envelope ( $h\nu$ , Figure 2A) affords a porphyrin-localized excited state [ $^1(\text{PMg})^*-\text{Q}$ ], which decays via a solvent-independent ET process to produce the charge-separated state ( $\text{P}^+\text{Mg}-\text{Q}^-$ ) on a time scale ( $\tau_{\text{CS}} = 350 \text{ fs}$ ) likely rate-limited by electronic population equilibration between the (porphyrinato)metal  $Q_x$  and  $Q_y$  levels.<sup>1</sup> Notably, the ET dynamics evinced for PZn–PI are pump wavelength independent within the Q-band spectral region (Figure 2B), indicating that no direct CT states are accessed over these excitation energies. These data suggest that a combination of diminished D–A electronic coupling and increased activation free energy in PZn–PI may be responsible for

- (17) Osuka, A.; Marumo, S.; Mataga, N.; Taniguchi, S.; Okada, T.; Yamazaki, I.; Nishimura, Y.; Ohno, T.; Nozaki, K. *J. Am. Chem. Soc.* **1996**, *118*, 155–168.
- (18) Imahori, H.; Yamada, K.; Hasegawa, M.; Taniguchi, S.; Okada, T.; Sakata, Y. *Angew. Chem., Int. Ed. Engl.* **1997**, *36*, 2626–2629.
- (19) Davis, W. B.; Svec, W. A.; Ratner, M. A.; Wasielewski, M. R. *Nature* **1998**, *396*, 60–63.
- (20) Staab, H. A.; Nikolic, S.; Krieger, C. *Eur. J. Org. Chem.* **1999**, 1459–1470.
- (21) Fajer, J.; Borg, D. C.; Forman, A.; Dolphin, D.; Felton, R. H. *J. Am. Chem. Soc.* **1970**, *92*, 3451–3459.

the observed differences in the excited-state dynamics relative to those elucidated for PMg–Q.

Computation of the driving force for charge separation ( $\Delta G_{CS}$ ) utilizing the Weller expression to estimate the ion pair destabilization energy of the CS state,<sup>22,23</sup> and approximation of the outer-sphere reorganization energy ( $\lambda_s$ ) using the classic Marcus expression,<sup>24,25</sup> provides some insight into the origin of the disparate CS dynamics observed for PMg–Q and PZn–PI. For PMg–Q, photoinduced ET is predicted to be nearly activationless ( $\Delta G_{CS} + \lambda_T = -0.07$  eV), congruent with the fact that the optical spectra for this species display a prominent low-energy CT transition.<sup>1</sup> In contrast, the analogous computed value of  $\Delta G_{CS} + \lambda_T$  for PZn–PI is 0.3 eV, consistent with the lack of an observable CT transition in its absorbance spectrum. Note also that the value of  $\Delta G_{CR} + \lambda_T \approx -0.60$  eV, indicating that inverted region effects play a role in diminishing the magnitude of  $k_{CR}$  with respect to  $k_{CS}$ .

Reduced D–A  $\pi$ -overlap relative to that evident for PMg–Q is an additional factor responsible for the observed porphyrin-localized nature of the PZn–PI Q states. MOPAC-determined dihedral angle-dependent relative heats of formation (Figure 3) reflect the enhanced steric barrier to libration about the PZn-to-PI bond with respect to analogous motions involving the PMg-to-quinonyl linkage. The energetic barrier to complete rotation about the D–A bond in PZn–PI was calculated<sup>26</sup> to be 41.0 kcal/mol (1.8 eV), while the analogous rotational barrier for PMg–Q was determined to be 33.5 kcal/mol (1.5 eV). Note that the surface describing the dihedral-

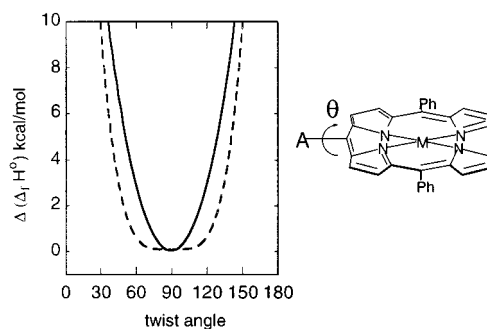


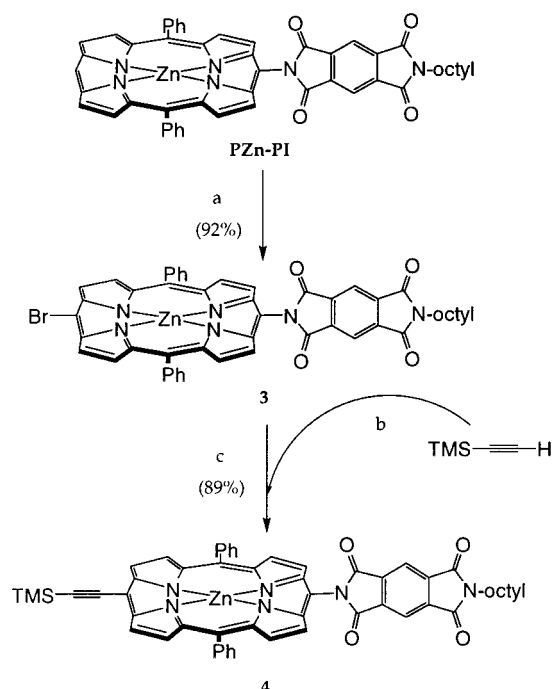
**Figure 3.** A comparison of computed relative heats of formation determined as a function of the twist angle ( $\theta$ ) between the (porphyrinato)-metal and acceptor least-squares planes for the PZn–PI (solid line) and PMg–Q (dotted line) D–A complexes. The heats of formation at angle  $\theta$  were calculated with the CAChe MOPAC application, version 94, using AM1 semiempirical Hamiltonians.

angle-dependent heat of formation for PMg–Q is shallow with respect to that determined for PZn–PI. PZn–PI structural conformers with D–A dihedral angles of  $90 \pm 15^\circ$  are computed to have heats of formation within 1 kcal/mol of that determined for the minimum-energy structure. In contrast, the structural heterogeneity of PMg–Q conformers possessing similar stability is more extensive; conformers having D–A dihedral angles of  $90 \pm 35^\circ$  are calculated to possess  $\Delta H_f$  values within 1 kcal of that of the minimum-energy structure. Because the extent of the  $\pi$ -conjugation between D and A affects the magnitude of the electronic coupling matrix element ( $H_{DA}$ ), augmented steric factors in the PZn–PI system would be expected to diminish D–A electronic communication and limit the degree of delocalization in the PZn–PI singlet excited state.

In contrast to many directly linked D–A compounds, further functionalization of PZn–PI is uncomplicated. *meso*-Halogenation of the porphyrin macrocycle is carried out regioselectively, in high yield and under facile conditions (Scheme 2). The halogenation product *N*-[5-(15-bromo-10,20-diphenylporphyrinato)zinc(II)]-*N'*-(octyl)pyromellitic diimide (**3**) can thus serve as a building block in the synthesis of more elaborate donor–spacer–acceptor assemblies that incorporate multiple light-absorbing D or A units. Because halogenated porphyrins are reactive substrates in Pd-catalyzed cross-coupling reactions,<sup>27–37</sup> **3** can be elaborated

- (22) The Gibbs energy for charge separation ( $\Delta G_{CS}$ ) was estimated using the equations  $-(\Delta G_{CS}) = E_{(0,0)}(MP) - E_{1/2}(MP/MP^+) + E_{1/2}(A^-/A) + \Delta G(\epsilon)$  and  $\Delta G(\epsilon) = e^2[(1/\epsilon_s)\{1/(2R_D) + 1/(2R_A) - 1/R_{DA}\} - (1/\epsilon_T)\{1/(2R_D) + 1/(2R_A)\}]$ , where  $E_{(0,0)}$  is the energy of the lowest excited singlet state (PZn–PI, 2.15 eV; PMg–Q, 2.05 eV),  $E_{1/2}(MP/MP^+)$  is the one-electron oxidation potential of the (porphyrinato)metal compound,  $E_{1/2}(A^-/A)$  is the one-electron reduction potential of the acceptor, and  $\epsilon_T$  is the static dielectric constant for the high dielectric solvent in which the potentiometric measurements were obtained.  $E_{1/2}(\text{PI}^-/\text{PI})$  and  $E_{1/2}(\text{ZnP/ZnP}^+)$  were determined by cyclic voltammetric experiments to be  $-0.88$  and  $0.85$  V vs SCE, respectively (see the Supporting Information).  $E_{1/2}(\text{Q}^-/\text{Q})$  and  $E_{1/2}(\text{MgP/MgP}^+)$  are respectively  $-0.6$  and  $0.74$  V vs SCE; these data are available from the literature (see: Carnieri, N.; Harriman, A. *Inorg. Chim. Acta* **1982**, 62, 103–107. Furhop, J.-H.; Mauzerall, D. *J. Am. Chem. Soc.* **1969**, 91, 4174–4181. Furhop, J.-H. *Z. Naturforsch.* **1970**, 25B, 255–265).
- (23) Weller, A. *Z. Phys. Chem. N. F.* **1983**, 133, 93–98.
- (24) Marcus, R. A. *J. Chem. Phys.* **1965**, 43, 679–701.
- (25) The solvent reorganization energy ( $\lambda_s$ ) and the total reorganization energy ( $\lambda_T$ ) were calculated using the equations  $\lambda_s = e^2/(4\pi\epsilon_0)\{1/(2R_D) + 1/(2R_A) - 1/R_{DA}\}[(1/\epsilon_{OP}) - (1/\epsilon_s)]$  and  $\lambda_T = \lambda_s + \lambda_i$ , where  $R_D$  is the radius of PZn and PMg (5.5 Å),  $R_A$  is the acceptor radius (PI, 4 Å; Q, 3.2 Å),  $R_{DA}$  is the center-to-center distance between the porphyrin and acceptor units (PMg–Q, 6.4 Å; PZn–PI, 8.5 Å), and  $\epsilon_{OP}$  and  $\epsilon_s$  are the optical and static dielectric constants, respectively. The inner-sphere reorganization energy ( $\lambda_i$ ) was calculated to be 0.3 eV, a value typical for D–A systems of this size (see, for example: Rubtsov, I. V.; Shirota, H.; Yoshihara, K. *J. Phys. Chem. A* **1999**, 103, 1801–1808).
- (26) Rotational barriers were calculated with the CAChe MOPAC application, version 94, using the AM1 semiempirical Hamiltonians. To check the accuracy of this computational study, a test calculation was performed on (10,20-diphenyl-15-cyclohexylporphyrinato)zinc(II); the theoretically predicted rotational barrier of the cyclohexyl group (14 kcal/mol) compared favorably with that evaluated experimentally ( $12 \pm 0.5$  kcal/mol). See: Veyrat, M.; Ramasseul, R.; Turowska-Tyrk, I.; Scheidt, W. R.; Autret, M.; Kadish, K. M.; Marchon, J.-C. *Inorg. Chem.* **1999**, 38, 1772–1779.

- (27) DiMaggio, S. G.; Lin, V. S.-Y.; Therien, M. J. *J. Am. Chem. Soc.* **1993**, 115, 2513–2515.
- (28) DiMaggio, S. G.; Lin, V. S.-Y.; Therien, M. J. *J. Org. Chem.* **1993**, 58, 5983–5993.
- (29) Lin, V. S.-Y.; DiMaggio, S. G.; Therien, M. J. *Science* **1994**, 264, 1105–1111.
- (30) LeCours, S. M.; DiMaggio, S. G.; Therien, M. J. *J. Am. Chem. Soc.* **1996**, 118, 11854–11864.
- (31) Hyslop, A. G.; Kellett, M. A.; Iovine, P. M.; Therien, M. J. *J. Am. Chem. Soc.* **1998**, 120, 12676–12677.
- (32) Gauler, R.; Risch, N. *Eur. J. Org. Chem.* **1998**, 1193–2000.
- (33) Blake, I. M.; Rees, L. H.; Claridge, T. D. W.; Anderson, H. L. *Angew. Chem., Int. Ed.* **2000**, 39, 1818–1821.
- (34) Deng, Y.; Chang, C. K.; Nocera, D. G. *Angew. Chem., Int. Ed.* **2000**, 39, 1066–1068.
- (35) Tse, M. K.; Zhou, Z.-Y.; Mak, T. C. W.; Chan, K. S. *Tetrahedron* **2000**, 56, 7779–7783.
- (36) Shi, X. L.; Amin, S. R.; Liebeskind, L. S. *J. Org. Chem.* **2000**, 65, 1650–1664.
- (37) Shanmugathasan, S.; Edwards, C.; Boyle, R. W. *Tetrahedron* **2000**, 56, 1025–1046.

Scheme 2<sup>a</sup>

<sup>a</sup> Conditions: (a) NBS, CH<sub>2</sub>Cl<sub>2</sub>, 0 °C; (b) *n*-BuLi, THF, −78 °C; ZnCl<sub>2</sub>, THF; (c) Pd(PPh<sub>3</sub>)<sub>4</sub>, THF, 65 °C.

straightforwardly at the 15-position. The conversion of **3** to *N*-{5-[15-(2-(triisopropylsilyl)ethynyl)-10,20-diphenylporphyrinato]zinc(II)}-*N'*-(octyl)pyromellitic diimide (**4**) (Scheme 2) illustrates this point.

## Conclusion

In summary, we have prepared a *meso*-pyromellitimide-substituted (porphyrinato)zinc(II) complex which undergoes ultrafast, photoinduced charge separation and thermal charge

recombination ET reactions. The ultrafast ET dynamics observed for PZn-PI in methylene chloride differ markedly from those delineated previously for closely related 5-quinonyl-elaborated porphyrin compounds, such as PMg-Q.<sup>1</sup> In PMg-Q, excitation into an *x*-polarized Q state produces directly a CT excited state, while excitation into a Q<sub>y</sub> absorption band produces a porphyrin-localized excited state which decays to the charge-separated state on a time scale ( $\tau_{CS}$  = 350 fs) controlled by population exchange between the Q<sub>x</sub> and Q<sub>y</sub> levels.<sup>1</sup> Due to diminished D-A electronic coupling and increased activation free energy relative to PMg-Q, low-lying CT states do not mix effectively with porphyrin-localized B and Q electronically excited states in PZn-PI. Charge separation dynamics in PZn-PI are thus pump wavelength independent, with the porphyrin-localized excited-state decaying to the charge-separated state on a time scale of 770 fs. Notably, the PZn-PI D-A complex can be further functionalized via halogenation and subsequent metal-catalyzed cross-coupling at the porphyrin *meso*-position *anti* to the PI moiety; we thus expect that this species will be a useful synthon in the preparation of more elaborate multi-chromophoric donor-acceptor arrays.

**Acknowledgment.** This work was supported by a grant from the Division of Chemical Sciences, Office of Basic Energy Research, U.S. Department of Energy (DE-FG02-94ER14494). M.J.T. thanks the Office of Naval Research (N00014-97-0317) and the MRSEC Program of the National Science Foundation (DMR-00-79909) for equipment grants for transient optical instrumentation.

**Supporting Information Available:** Absorption and emission spectra as well as cyclic voltammetric data. This material is available free of charge via the Internet at <http://pubs.acs.org>.

IC0108641